ISSN 1330-3651 (Print), ISSN 1848-6339 (Online) https://doi.org/10.17559/TV-20220912160544
Original scientific paper

Performance Evaluation of Novel Rare Earth Free Magnets Based Motors for Electric Vehicle Applications

Sundaramahalingam SUBRAMANIAM*, Manikandan Bairavan VEERAYAN

Abstract: Electrical Vehicles (EVs) are regarded as an effective solution in a world where environmental protection along with energy crises is gaining higher attention. Permanent Magnet Synchronous Machines (PMSMs) are considered significant competitors for EVs amongst the other varied motor drives. Owing to their higher efficiency, higher output power to volume ratio, and higher torque to current ratio, they are regarded as a feasible option in several sorts of applications like wind turbines, along with EVs. For higher-performance applications, Permanent Magnet (PM) motors with Rare-Earth (RE) magnets are pondered as one of the best candidates. Conversely, replacing the Rare-Earth (Neodymium-iron-boron) in EVs with lesser or even no RE alternatives is the most critical concern in PM owing to their limited along with the unstable supply of RE elements. Therefore, to eliminate the usage of RE magnets as well as to identify the finest alternative materials, which assure lower cost along with mass production in manufacturing industries, various permanent magnetic materials are examined here with different PMSM designs for EVs applications. Manganese Aluminide (MnAl), Ferrite, Tetrataenite ($L_{10}FeNi$), Iron Nitride ($Fe_{16}N_2$) and Nanocomposite magnetic materials are the varied magnetic materials utilized for evaluation. For varied magnetic materials, the simulation outcomes are obtained regarding the variations in cogging torque, average torque, efficiency, along with magnet mass. On analogizing RE with various magnetic materials, it was established that a higher performance was attained by replacing RE magnets with substitute magnetic material; in addition, it also proves to be highly effective. It is observed that although their electromagnetic performance of the various materials is similar, iron nitrade has an excellent demagnetization withstand capability. Finally, in contrast to the interior V type with rare earth magnets, iron nitrade and MnAl magnet machine can attain better torque development with high efficiency.

Keywords: Electric Vehicles (EV); Ferrites; magnetic materials; neodymium-iron-boron; Permanent Magnet Synchronous Machine (PMSM); PMSM design; Rare-Earth (RE) magnets

1 INTRODUCTION

Recently, the contradiction between the deficiency of oil and environmental pollution is turning into a severe concern owing to the rapid enlargement of the global conventional fuel vehicle industry [1]. The governments of several countries have made gradually more strict emissions regulations to protect the environment of the worsening environmental pollution together with the fossil fuel supply [2]. Global warming and high pollution levels require more intensive usage of green and renewable energy sources. For transport, one of the solutions is increased electrification of the powertrain as can be found in hybrid, plug-in hybrid, and pure electric vehicles. For the development of EVs, a greater effort has been put forward by governments, academics, along with industrial communities to overcome issues like energy shortages, global warming, and noise pollution pertinent to conventional vehicles [3]. Motors are the unique source of propulsion in EVs. Better torque characteristics in the lower-speed range, as well as better flux-weakening ability in the higher-speed range, is required for the motors intended for EVs [4]. Higher power density and higher efficacy with an effective heat loss to the surroundings are the beneficial factors in the PMSM; thus, it is a better candidate for EV applications [5]. PMSM has strategic significance in the modeling, along with the design of electrical, mechanical, electronic, together with mechatronic systems; as a result, it has gained attention among researchers [6]. In the PMSM, the dual closed-loop structure is espoused where the inner loop is the current loop; in addition, the outer loop is the speed loop; furthermore, to control the PMSM, the linear control, like the PI control methodology, is utilized [7]. However, the PMSMs' dynamic model is highly nonlinear together with strongly coupled; in addition, owing to uncertainties like load disturbances, the motor system could be disturbed [8]. Regarding the specific application, numerous sorts of PMSM have been developed. By making slight alterations in the design of the rotor, stator, magnet types, along with windings types, an enhanced performance could be obtained. (i) Surface PMSM (SPMSM), and (ii) Interior PMSM (IPMSM) are the two types of PMSM regarding the rotor structure [9-10]. A faster dynamic response along with a smaller torque ripple was owned by the conventional SPMSM; however, it has a lower power density. Similarly, a higher power density along with a stronger overload capacity was owned by the conventional IPMSM; nevertheless, it has a larger leakage flux [11]. Higher efficiency, higher reliability, higher power/torque density, and better field weakening performance are the attractive advantages possessed by the IPMSM. Therefore, in various industrial applications like EVs, and robot motion control, along with other industrial fields, the IPMSM has been utilized [12]. Most IPMSM has permanent magnets in the rotor, which are often made of rare earth magnets like Neodymium-iron-boron (NdFeB). Because powered coils require electricity to be transferred from the battery to the coils in a spinning rotor, it is great to have a persistent source of powerful rare earth magnetism in the rotor. Permanent magnets, on the other hand, come with their own set of problems. China produces 97% of the world's rare earth magnets, and governmental control over such a critical resource for a variety of high-tech businesses has been a severe concern in the past. The utilization of expensive RE-PMs is the major limitation of a higher-performance IPMSM [13]. By delivering better performance under stringent driving conditions, the RE magnets like neodymium and dysprosium have turned into a choice for traction motors [14]. Nevertheless, in a few years, the price and availability of these materials will possibly turn into an issue [15]. In 2018, 93% of all the EVs produced in the world had a powertrain driven by permanent magnet motors made up of rare earth magnets. Several companies, like BMW, Audi, Renault, and others, are currently producing electric motors without magnets,

while others are looking into new technologies. Thus, Less-Rare-Earth IPMSM (LRE-IPMSM), which utilizes larger reluctance torque and mitigates the consumption of RE materials, is considered an alternative [16]. Therefore, to minimize the amount of RE magnets by substituting RE-PM with non-RE-PM like Ferrite PM (Fe-PM), PM-assisted SynRM (PMaSynRM), along with Synchronous Reluctance Motor (SynRM), various types of research have been conducted [17]. Substituting PMSMs with varied permanent magnetic materials in lower-speed and higher-torque applications is especially interesting owing to their higher RE-PM content. A considerable cost reduction can be engendered by eliminating the expensive magnet material [18]. Maria Hernandez et al. [19] developed a Life Cycle Assessment (LCA) of the traditional traction electric motor along with the substitution of its RE-PM by a Fe-PM. To evaluate flows of mass along with energy and their environmental consequences across the life cycle from raw materials extraction to the end-of-life stage, the LCA model was well-suited. To analogize environmental profiles and probable enhancement strategies, alternative motor efficiency situations were evaluated. The outcomes displayed that to enhance the motor's environmental performance over the RE magnets together with mitigating the risk along the supply chain of raw materials aimed at the magnets, the Ferrite Magnet was established as an appropriate alternative. Michele De Gennaro et al. [20] presented the prototyping, designing, along with testing results of a PMaSynRM, apt for A/B-segment EVs. The machine was designed in such a manner to avoid the usage of RE material in the magnets; thus, by implementing ferrite with a hairpin winding for the stator together with a lightweight modular design for the rotor, the performance loss was reimbursed. This methodology also presented the design of the full drive with incorporated power electronics along with an air-cooled housing, apart from the motor itself. The simulation outcomes displayed that a maximum torque performance was provided by the drive bringing about the best-in-class ferrite-centric PMaSynRM. Nevertheless, the environmental damage sourced from the enhanced traditional designs of electric motors was not evaluated in this assessment. Chae-Lim Jeong et al. [21] introduced an optimized design of PMSM utilizing hybrid-type PM to enhance the output characteristics together with reliability. Here, utilization of both Neodymium PM (Nd-PM) and Fe-PM in a rotor is proffered as the hybrid type PM. Initially, by pondering magnetic equivalent circuits along with applying magnet characteristics of Fe-PM altered by the reversed flux of Nd-PM, the basic design of PMSM was conducted. A parallel configuration of reluctance factors was utilized aimed at optimizing the motor by employing hybrid-type PM, thus augmenting output characteristics. Furthermore, a Finite Element Method (FEM) was utilized to evaluate it. The performances of the target and presented motors were analogized using FEM. The experiential outcomes displayed that when analogized with the target motor, the presented motor provided better performance. However, this motor could suffer inadequately at a higher temperature. Jong-Hyeon Woo et al. [22] recognized the probability of higher-speed PM motors in which RE magnets were substituted by FMs, by pondering the current harmonics. Regarding the current harmonics, the electromagnetic characteristics of a higher-speed motor with RE along with Fe-PMs were evaluated. By comparing the manufactured models' experimental outcomes, the findings were verified. It was established that to assess higher-speed PMSM analysis, the electromagnetic loss analysis methodology subsuming the harmonics of the current was essential. Furthermore, the RE magnet-centered motor was replaced by the FM motor. The development of high-speed Fe-PM motors for several applications was contributed by the presented analysis methodology. However, the motor performance was affected since the FMs could effortlessly collide with other metals. Xiaoyong Zhu et al. [23] presented an LRE-PM brushless motor with two types of PM materials for mitigating the consumption of RE-PM material. In this, to form the hybrid PM excitation, the RE-PM was intentionally amalgamated with non-RE ferrite PM. A multi-objective stratified optimization technique was developed to design the presented motor effectually; in this technique, the five optimization objectives (output torque, torque ripple, PM cost, cogging torque, together with efficiency) being selected were partitioned into two levels. After that, to satisfy specific design requirements, various optimization methodologies were skilfully amalgamated. Then, the respective electromagnetic performances were assessed along with contrasted with the conventional RE-PM brushless motor. The presented motor and the optimization model's feasibility along with validity were verified by analyzing the experimental outcomes. In comparison to a present electric vehicle, manufacturer of electric motor is looking for the improved performance in terms of specific power, power density, and efficiency. However, the cost of Rare earth permanent magnet material expenses at least 40% of the final electric motor prices. In order to achieve cost-effective Electric vehicle markets and expand the EV markets globally, manufacturers and suppliers of the electric vehicles around the world look into alternative non-RE motor technologies. This paper aims to contribute to the development of a new generation of electric drive trains that avoid the usage of rare-earth magnets while maintaining industrial feasibility for mass production and focusing on low-cost manufacturing technologies. Therefore, the development of alternative non-RE motor technologies is an essential key concern in future economic stability to attain green energy goals & non polluted environments. Consequently, to eliminate the usage of RE-PM and select substitute materials for the development of EVs, various permanent magnetic materials with different PMSM designs are analyzed in this paper. The proposed rare-earth free elements and nanocomposite magnetic materials will be a good replacement for the existing rare-earth magnetic materials in these applications. Overall, this paper describes the merits and demerits of each alternative to substitute rare-earth PM motors. The paper's remaining parts are structured as the proposed framework is explicated in section 2; the model is investigated with various materials in section 3; lastly, the paper is winded up in section 4.

2 RESEARCH METHODOLOGY

In a growing number of applications, PMSM has gained a foothold. Owing to its higher power/torque density along with higher efficiency, it has been extensively utilized as the driving core in EVs. The demands of the motor utilized for the EVs comprising higher efficiency, higher torque density, a wider speed range, together with higher power factor are satisfied by the RE-PMs in PMSMs. Nonetheless, the LRE- IPMSM utilized for EVs has gained higher attention since the price of RE-PM fluctuates dramatically. Thus, for EV application, the effect of various permanent magnetic materials with different PMSM designs has been analyzed here. Primarily, the PMSM's design is explicated; then, by utilizing Neodymium-iron-boron (NdFeB) RE magnets with varied magnetic materials like Ferrite, Manganese Aluminide, Iron Nitride, Tetrataenite along with Nanocomposite magnetic materials, the PMSM's electromagnetic analysis is performed. After that, for effective assessment, the electromagnetic analysis along with its comparisons is made.

2.1 Design of PMSM

Higher torque-to-current ratio, higher power-to-weight ratio, higher efficiency and robustness are provided by PMSM potentially. In the latest variable speed AC drive, especially in EV applications, the PMSMs are utilized commonly owing to the aforementioned favourable points. On the rotor core, which has a similar role as field winding in a synchronous motor, the PMs are mounted. Regarding the PM mounting in the rotor, the PMSM is categorized as: (i) Surface mounted PMSM and (ii) IPMSM. Fig. 1 exhibits the structure of both PMSMs.

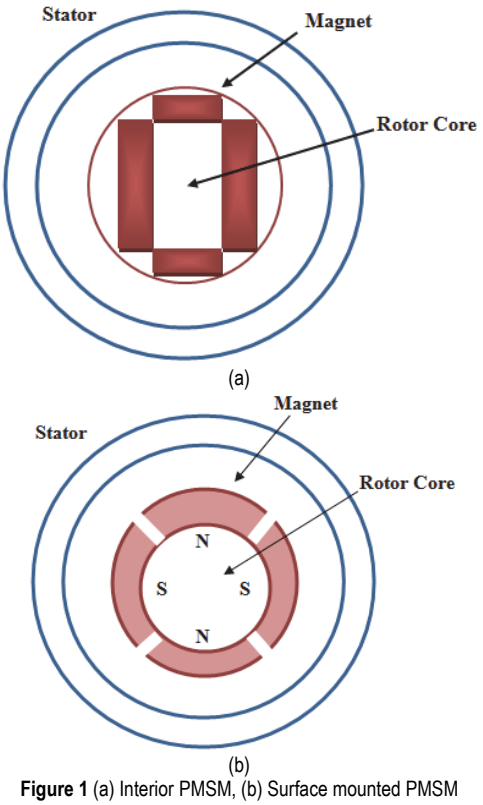

Figure 1 (a) Interior PMSM, (b) Surface mounted PMSM

In this study, constant speed Permanent Magnet Synchronous Motor is designed based on the required power applications. The stator and rotor dimensions are calculated and presented in Tab. 1.

Table 1 Specifications of proposed PMSM for electric vehicle applications

Parameters	Values
Maximum Power / kW	100 kW
No-load phase voltage at rated speed / rms	2042 V
Rated Torque / Nm	245 Nm
Rated Speed / rpm	10000 rpm
Number of Poles	8
Number of Stator Slots	24
Number of Rotor bars	4
Stator Inner Diameter / mm	117 mm
Stator Outer Diameter / mm	200 mm
Air Gap Width / mm	0.8 mm
Stator Length / mm	69 mm
Rotor Outer Diameter / mm	115mm
Rotor Inner Diameter / mm	95 mm
Slot Depth	29.2 mm
Slot Width	14.5 mm

2.2 Different Rotor Topologies of PMSM

In most machines, the stator design is similar in nature; conversely, to make the machine unique for various applications, the rotor structure might get varied. Principally, in estimating the PMSM's efficiency, a major role is performed by the PM rotor orientation, dimension, along with air gap length. Thus, the different rotor topologies [24] like surface PM rotor, decentred PM rotor, broad loaf PM rotor, Spoke PM rotor, Interior PM Rotor, and stator configuration of PM rotor for various PMs are investigated in this section. The steel material with grade of M350-50A is utilized for stator and rotor. 3-phase, 56 turns lap winding type is preferred as the stator winding. Fig. 2 demonstrates the PMSM's different rotor topological structures.

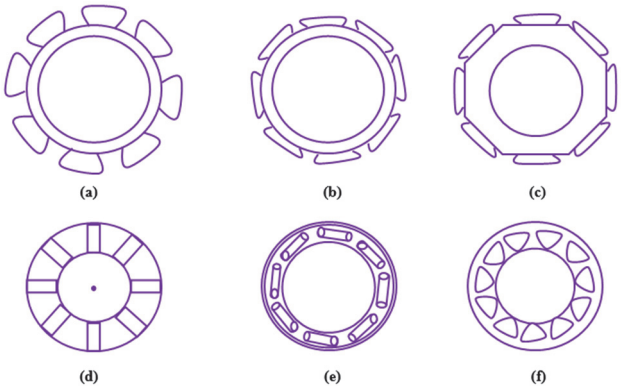

Figure 2 Cross-section of different rotor topologies (a) surface PM rotor, (b) decentred PM rotor, (c) broad loaf PM rotor, (d) Spoke PM rotor, (e) Spoke PM rotor, and (f) stator configuration of PM rotor

2.3 Different Permanent Magnetic Materials

Permanent magnets (PM) are increasingly being used in renewable energy devices such as electric vehicle (EV) motors and wind turbine generators. The characteristics of a permanent magnet are obtained by the product of remanent flux density (B_r) and coercivity (H_{ci}). Due to the high maximum energy product $(BH)_{max}$ of rare-earth permanent magnets, an interior permanent magnet synchronous motor is commonly employed for electric

vehicle applications. The $(BH)_{max}$ determines the torque and power density of a motor and coercivity decides the demagnetization property of the magnets. As a result, a high $(BH)_{max}$ and coercivity are desirable. Despite the fact that rare-earth permanent magnets have a high $(BH)_{max}$, recent price and supply variations of rare earth elements become issues on electric machines production at fixed low cost with reliable supply. The scarcity of rare-earth (RE) elements and the low operating temperature of Nd-Fe-B, on the other hand, are major concerns. RE-free PM recently has received a great attention. Commercially, the various hard magnetic materials are developed and their properties are shown in Fig. 3. The RE-free PMs, such as τ-MnAl, LTP-MnBi, Alnico, SmCo produce moderate $(BH)_{max}$ in 3 - 11 MGOe. Accordingly, it is proposed to develop non-RE permanent magnets PMs with higher $(BH)_{max}$ than that of currently available non-RE PM using nano composite magnets to fill the gap between 10 and 20 MGOe. In this study, five alternative permanent magnetic material types are chosen for replacing the RE-PMSM. The alternatives being chosen are Ferrite, Manganese Aluminide (MnAl), Iron Nitride ($Fe_{16}N_2$), Tetrataenite (L_{10}-FeNi), and Nanocomposite Magnetic materials.

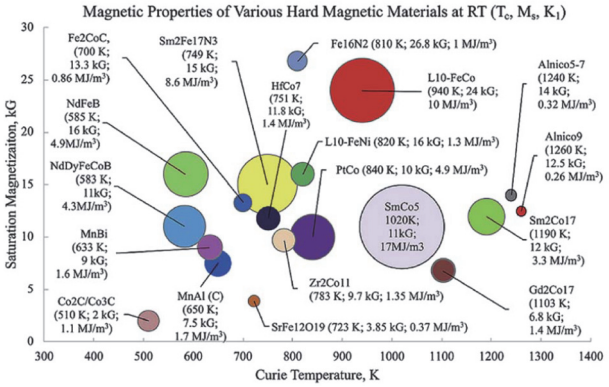

Figure 3 Properties of various hard magnetic materials [25]

NdFeB [26] is the most extensively utilized RE magnet. To form NdFeB magnetic materials, the NdFeB, which is composed of an alloy of neodymium, iron, along with boron, is utilized. The materials included in the manufacturing of NdFeB are considerably inexpensive; thus, the NdFeB is utilized as a substitute for RE magnets in PMSM. The NdFeB's crystal structure along with symmetry demonstrates symmetry in both orthogonal planes; in addition, it contributes to its robust magnetic properties. The NdFeB has a tetragonal structure. A magnetization of around 1.6 T at room temperature is produced by this symmetry; it also produces anisotropy brought about from the 'mm' symmetry via the '2' neodymium sites. By controlling the size, shape, along with orientation of the grains, the magnetization and demagnetization of NdFeB are varied. Powdered metallurgical methodologies, sintering and melt spinning, and mechanical alloying are '3' varied processing models being employed currently to attain different microstructures.

While designing lower-cost non-RE EVs, Ferrite [27], the least expensive PMs, display capable opportunities. Various oxides with iron oxide are utilized as the major component in composing Ferrites, which are magnetic oxide compounds. Ferrites are ceramics that are made by amalgamating iron oxide (Fe_2O_3, rust) with small ratios of one or more metallic elements. A higher electrical resistivity is possessed by these ceramic materials; similarly, they also possess lower eddy-current losses. Regarding the crystal structure or the magnetic properties, these materials are classified into '2' groups. Hard ferrites are hard to demagnetize since they possess higher distinguished coercivity. Soft ferrites can easily alter their magnetization since they possess lower distinguished coercivity; accordingly, they can work as conductors of magnetic fields. To fabricate effective magnetic cores, soft ferrites are utilized. Manganese metal is antiferromagnetic; however, it can be a strong ferromagnet when alloyed with other elements. Owing to larger magnetic anisotropy energy, higher magnetic moment, higher Curie temperature, along with lower cost, the ferromagnetic phase of MnAl alloy utilized for the substitution of RE-PMs in PMSM for EV application turns extremely attractive. By inducing high purity Manganese (Mn) and Aluminium (Al) elements at a higher purity argon atmosphere, the MnAlPM [28] is formed. In general, for magnetic properties, the key factors are the phase composition and microstructure of MnAl alloys. Stronger magnetocrystalline anisotropy, good corrosion resistance, and lower density are contained in this magnetic material; in addition, the main components like Mn and Al are plentifully available in nature. At 51 - 58% Mn, the metastable MnAl compound with the tetragonal structure is formed. The ferromagnetic composition range from 50 to 60% Mn with a temperature of about 650 K; moreover, the compound's theoretical energy product is 112 kJ/m^3.For the applications of transformers, inductors, motors, generators, actuators, and sensors, Fe-based alloys are the extensively utilized magnetic materials. Here, Iron Nitride ($Fe_{16}N_2$) [29] centric magnetic material is utilized. It yields environment-friendly raw materials having saturation Magnetic Flux density (2.9 T), as well as reasonably higher magnetic anisotropy constant (1.8 MJ/m^3); thus, it is regarded as the most promising RE-free magnet candidate. To avoid of heavy RE elements, these materials are formed of merely light along with inexpensive elements, Fe and N. The coercivity temperature coefficient (~ 0.4 Oe/°C) of this material is in the range of 27 - 152 °C. The iron nitride magnet has a lower temperature (< 1500 °C) and lower coercivity; thus, they are highly significant. A hexagonal close-packed structure was possessed by the ferromagnetic iron nitrides. Furthermore, it is composed in the range of $-0.40 < x < 0.48$; in addition, it is a face-centered cubic, which has a ferromagnetic state under its Curie temperature of about 760 K. Owing to the larger magnetization of materials, the $Fe_{16}N_2$, which does not subsume any costly RE elements, exhibits potentially higher magnetic performance.

Being a PM free of RE elements, the Tetrataenite (L_{10}-FeNi) [30] is a promising candidate owing to its favourable properties. For the production of hard magnetic materials, a greater perspective was possessed by the Tetrataenite material, which is a RE-free PM brought on by neutron irradiation and annealed at 593 K under a magnetic field with a tetragonal crystal structure. Alternating layers of Fe and Ni atoms were contained in the tetragonal

structure; they were stacked in the direction parallel to the tetragonal c-axis. It has permanent magnetization properties with higher coercivity. Only in meteorites, the L_{10}-FeNi magnetic material is found. Lower thermal resistance along with the risk of depleting sources was possessed by these RE-free PMs. In iron meteorites, minute quantities of L_{10}-FeNi are subsumed. Subsequently, it has higher uniaxial magnetic anisotropy even though it includes common elements like Fe and Ni. The L_{10}-FeNi's saturation Magnetic flux density is 1.6T (154 A·m^2/kg), which is relatable to that of Nd-Fe-B. When analogized with the traditional magnets, a higher curie point of 550 °C was obtained. Consequently, L_{10}-FeNi is implemented as a PM; furthermore, to analyze its basic fundamental properties, in addition, to forge artificial synthesis methodologies, various experiments have been conducted. Nanocomposite with permanent magnetic is novel material. It consists of exchange coupled hard and soft magnetic material to obtain the large magnetic energy product and remanence. During the process of making nanocomposite magnets, the sizes of both the hard and soft phases are chosen in the nano scale ranges so that their magnetic moments of hard phase and soft phase materials are exchange coupled. Theoretical magnetic energy product of nano composite permanent magnet can be obtained as 1 MJ/m^3 due to mixture of a soft magnetic phase with its high saturation magnetization and hard-magnetic phase with its large magnetic anisotropy. Several researchers examine the possibility of making the excellent properties which are suitable for various permanent magnet applications. In this study, the properties of nano composite material $BaFe_{12}O_{19}/CoFe_2O_4$ are used. Although barium hexaferrite ($BaFe_{12}O_{19}$) has the properties of low density, high electrical resistivity, high saturation magnetization, and a large coercivity, it is not recommended to use this hard ferromagnet directly in any applications due to low energy product. In alternate ways, Cobalt ferrite ($CoFe_2O_4$) is one of the soft magnets which is characterized by its high magnetic anisotropy, saturation magnetization, and is chemically stable. The combination of these hard and soft materials will make improvement in magnetic properties of exchange-coupled nanocomposite. Such material is a good candidate with high saturation magnetization and large energy product $(BH)_{max}$ [31], which are larger compared with those of single magnetic-phase magnets.

3 RESULTS AND DISCUSSION

Here, to demonstrate the PMSM's effectiveness, the proposed magnetic materials' performance was analyzed with various PMSM designs for EV applications. ANSYS MOTORCOD is utilized for simulating the proposed research methodology. Tab. 2 exhibits the above-mentioned magnetic materials' general properties forge.

3.1 Electromagnetic Analysis of Different PMSM Rotor Structures

In order to obtain the fair comparison of the five different PMSM rotor designs, two dimensional design of the motor is modelled with same geometry, materials and ratings to achieve a wide range of constant power applications.

Table 2 Properties of different magnetic materials

Properties	NdFeB [26]	Ferrite [27]	MnAl [28]	Fe_{162} [29]	L_{10}-FeNi [30]	$BaFe_{12}O_{19}/CoFe_2O_4$ [31]
Maximum energy product BH_{max} / kJ/m^3	385	36	112	160	320	246
Curie Temperature T_c / K	312	450	650	810	810	785
Saturation magnetization M_s / MA/m	1.273	0.5	0.6	2.25	1.69	1.69
Magneto-crystalline anisotropy constant K_1 / MJ/m^3	5	8	1.78	2	1.3	3.45

The surface permanent machine type has low inductance and poor flux weakening capability. Due to its performance capability, interior PM machines are considered as good options to satisfy the performance of electric vehicle in all aspects. Cogging torque is the torque required to overcome the opposing torque produced by the magnetic attractive force between magnets on the rotor and the stator steel. There are multiple rotor positions within a revolution where the cogging torque is high. The peak cogging torque and average output torque versus rotor position angle for comparisons are shown in Fig. 4 and Fig. 5, respectively. It is shown that Interior V type and broad loaf type are having lesser cogging torque as compared with other topologies. The surface PM and Decentered PM are relatively high cogging torque at rated current. Similarly, the average torque produced by interior V type is better than other rotor topologies.

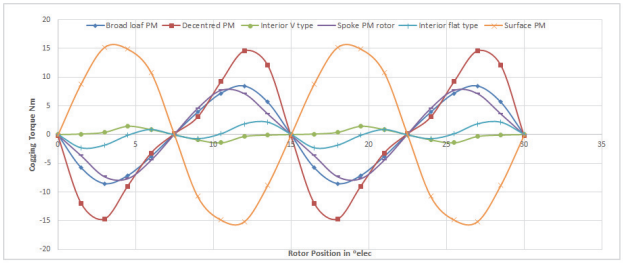

Figure 4 Comparison of the cogging torque of various rotor structures

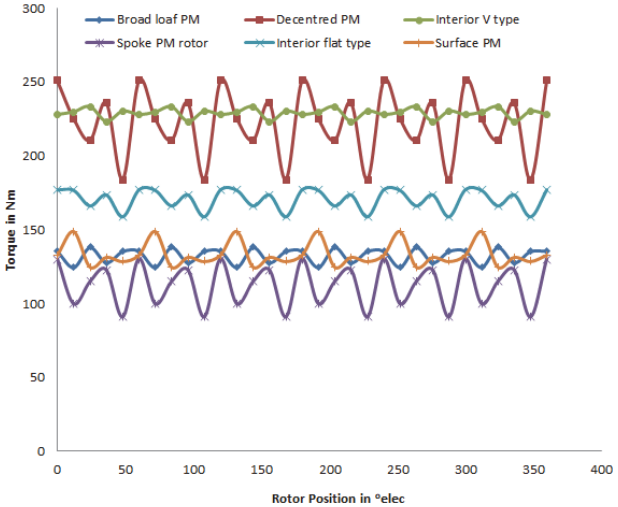

Figure 5 Comparison of the torque of various rotor structures

3.2 Electromagnetic Analysis of Different Materials

This section elaborates on the electromagnetic analysis of the proposed '5' alternative permanent magnetic material sorts of PMSM. Fig. 6 displays the structural design of such magnetic materials-based PMSM.

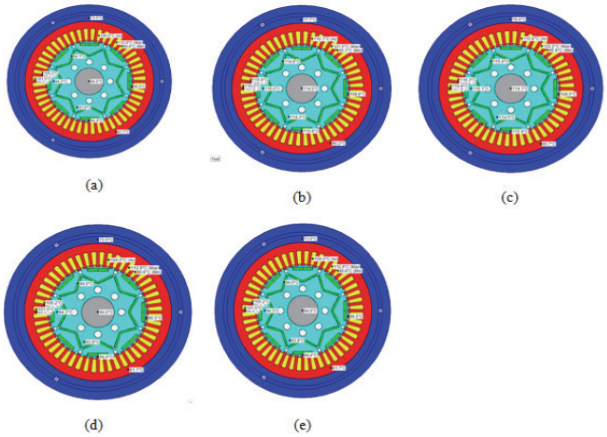

Figure 6 Structure of PMSM with alternate magnetic materials (a) Ferrite, (b) MnAl, (c) $Fe_{16}N_2$, (d) L_{10}-FeNi, and (e) Nano composite magnet

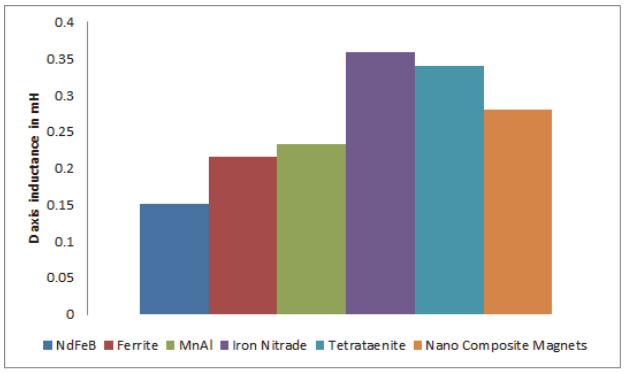

(a)

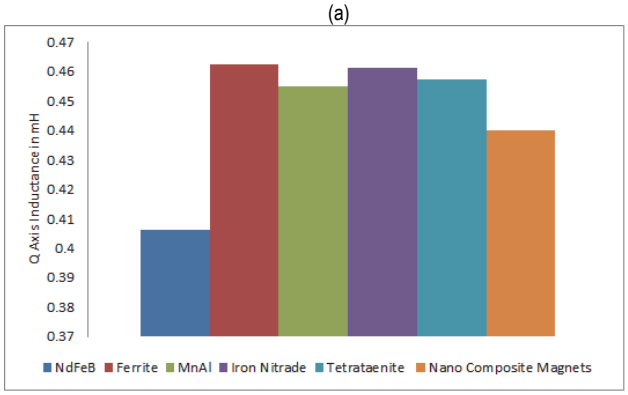

(b)

Figure 7 Comparison of the inductance of alternative magnetic materials for (a) d -axes and (b) q-axes

Fig. 7 graphically demonstrates the overall inductance comparison of q and d axes for varied magnetic materials. With magnetic materials like NdFeB, Ferrite, MnAl, Iron nitride, and L_{10}FeNi, the PMSM's inductance was represented in the above figure. The lower inductance of NdFeB shows that the characteristic current is higher than the rated current; thus, limiting the constant power speed range. Higher inductance was shown by iron nitride material in *d*-axes. Hence, iron nitride magnetic material's power speed in PMSM was highly more effective than others. When analogized with other materials, a better inductance with higher power speed was represented by the ferrite along with iron nitride materials in *q*-axes. From an electromagnetic point of view, the proposed models' behaviour is estimated. Magnetic flux density is an important parameter in permanent magnet motor design. The output power and efficiency of the machine increase by increasing the magnetic flux density. For this evaluation, the Magnetic flux density and Magnetic flux line maps are considered.

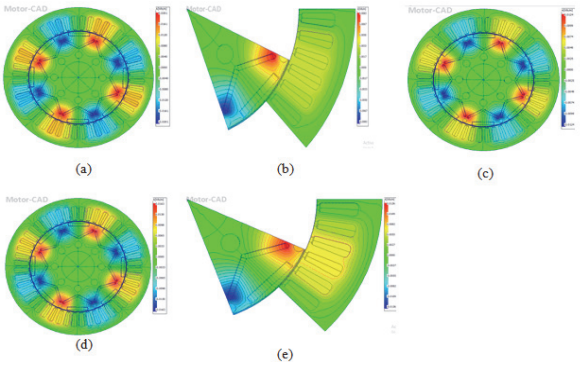

Figure 8 Magnetic flux density maps of (a) Ferrite, (b) MnAl, (c) $Fe_{16}N_2$, (d) L_{10}-FeNi, and (e) Nano composite magnet

The Magnetic flux density of various permanent magnetic materials, which are selected for replacing the RE magnets in PMSM for EV applications, is exhibited in Fig. 8. The material's magnetic thickness affects the Magnetic flux density, torque along with efficiency in various rotor topologies and magnetic materials.

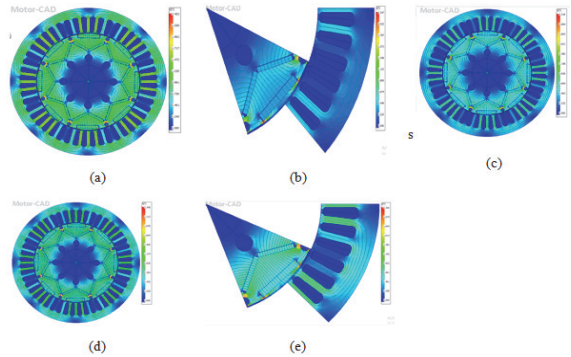

Figure 9 Magnetic flux lines of (a) Ferrite, (b) MnAl, (c) $Fe_{16}N_2$, (d) L10-FeNi, and (e) Nano composite magnet

The Magnetic flux lines of Ferrite, MnAl, $Fe_{16}N_2$, L_{10}-FeNi and Nano composite magnet materials are represented in Fig. 9. The number of magnetic field lines passing via the provided closed surface is proffered as magnetic flux lines. In this, the total magnetic field that passes via the given surface region is measured. Although curie temperature of the alternative materials is high as compared to the RE magnet materials, demagnetization may be attained due to low coercivity. Demagnetization is analysed for the machine at operating temperatures 100 °C and 40 °C with d axis currents. By doing coupled electromagnetic and thermal analysis on machine, demagnetization effects are analysed as shown in Fig. 10. It is observed that temperature affects the coercivity which leads the demagnetization easily.

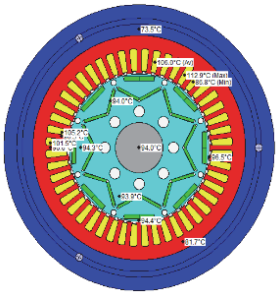

Figure 10 Temperature distribution in various parts of the machine

3.3 Characteristics Maps and Performance Evaluation

For evaluating the proposed design's efficiency, the efficiency variation and the efficiency of alternate RE-free magnetic materials in the desired torque-speed range are analysed.

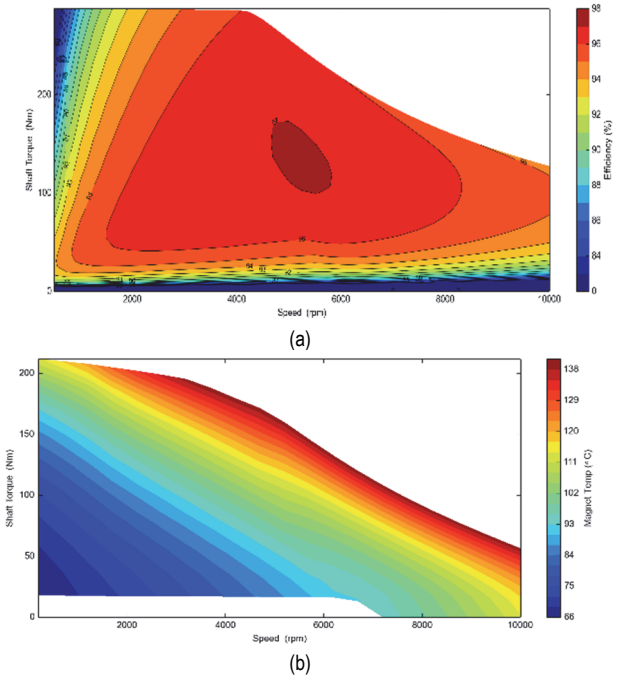

Figure 11 Performance maps of designed PMSM with NdFeB (a) efficiency map, and (b) temperature

According to Fig. 11a, for a larger zone in the torque-speed plane, the efficiency value is established to be well near 90%. The torque ripple differs as of higher torque, lower-speed region to lower torque, and higher-speed region of operation. As per Fig. 11b, in the torque-speed plane, the designed NdFeBPMSM's temperature range varies in the range of 84 ºC. The figures below show the performance maps of Ferrite PMSM regarding efficiency together with temperature.

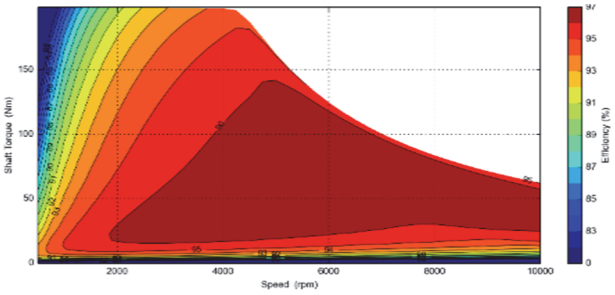

Figure 12 Performance maps of designed PMSM with ferrite

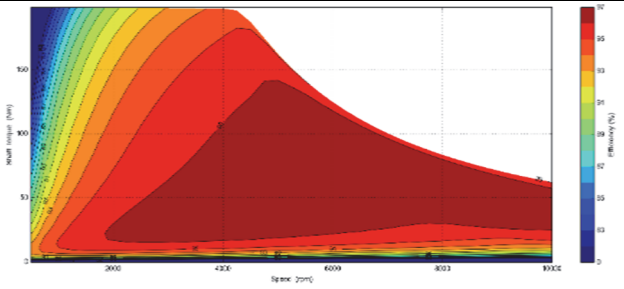

Figure 13 Performance maps of designed PMSM with MnAl

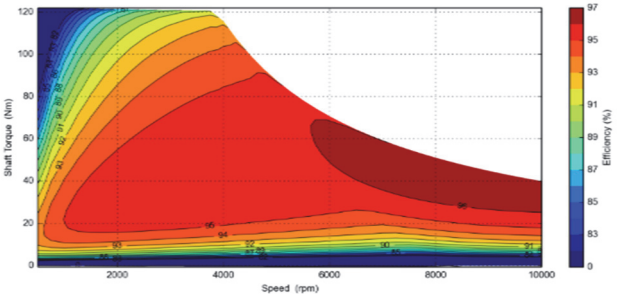

Figure 14 Performance maps of designed PMSM with $Fe_{16}N_2$

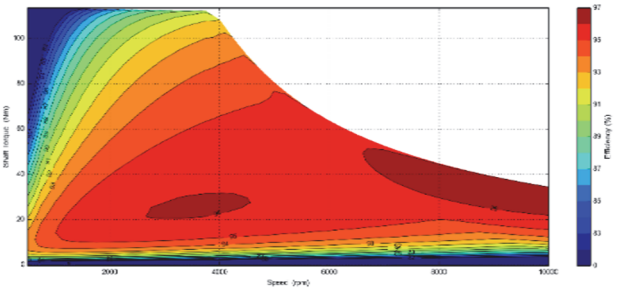

Figure 15 Performance maps of designed PMSM with L_{10}-FeNi

For materials like Ferrite, MnAl, $Fe_{16}N_2$, and L_{10}-FeNi, the efficiency variations in the required torque speed are depicted from Fig. 11 to Fig. 15 respectively. To identify the effectual substitute for RE magnets for PMSM in EV applications, the efficiency maps of several magnetic materials are provided. Therefore, the ferrite material's efficiency is between 85 - 87%. Similarly, in the desired torque-speed range, the MnAl magnetic material's efficiency is between 85 - 87%. For varying speeds along with torques, the $Fe_{16}N_2$ attained torque-speed efficiency in the range of 86 - 87%. In addition, the material's efficacy is about 85% for L_{10}-FeNi. After that, a temperature of around 82 ºC was exhibited by the ferrite material regarding the torque-speed temperature. In the same way, for varying torque-speed ranges, the temperature of MnAl, $Fe_{16}N_2$, and L_{10}-FeNi varies in the range of 84 - 93%, above 93%, and between 90 - 94%, respectively. Thus, for PMSM in EV applications, the material with lower magnetic temperature and higher efficiency turns into an apt substitute.

3.4 PerformanceA of Torque with Different Magnets

The figures below demonstrated the torque, cogging torque, and torque ripple comparisons of various magnetic materials.

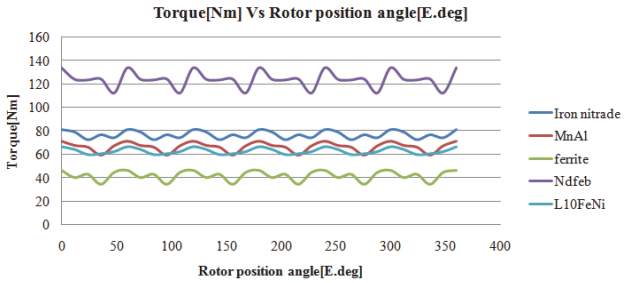

Figure 16 Torque vs rotor position angle

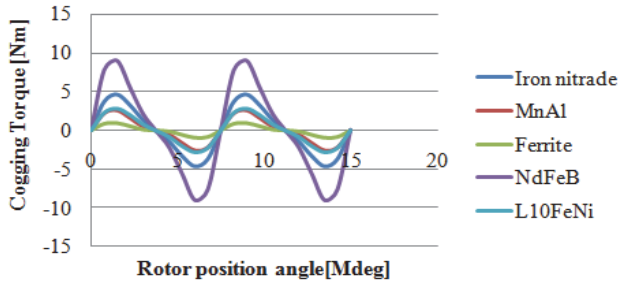

Figure 17 Cogging torque vs rotor position angle

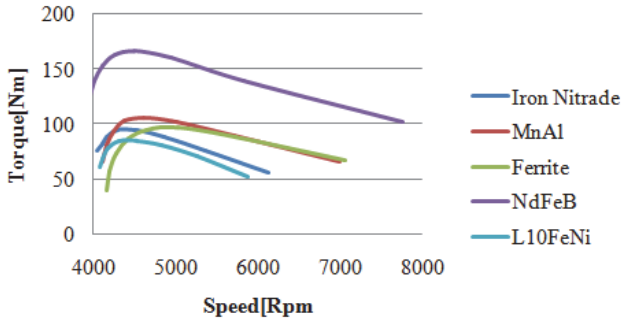

Figure 18 Torque vs speed

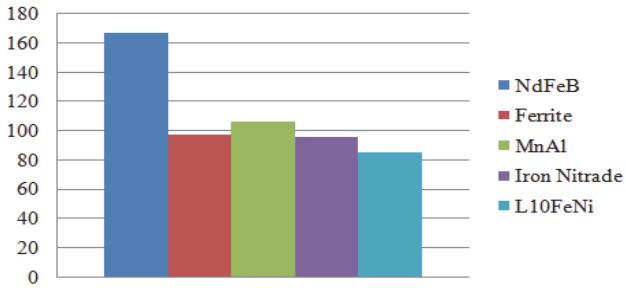

Figure 19 Maximum torque

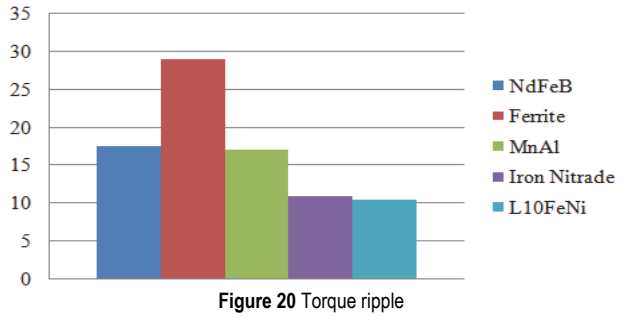

Figure 20 Torque ripple

A material with at least 30% of higher cogging torques will be highly competitive for the lower cost along with larger torque applications as shown in Fig. 16 and Fig. 17. Though higher cost, the magnets will offer almost the same levels of torque along with lower cogging ones for the required applications whilst operating in environments with higher temperatures. Likewise, a relatively better solution will be provided by the NdFeB magnet if the cost along with the cogging effect is a major concern. The torque and power versus speed performance at the rated current of the machine are plotted in Fig. 18. This shows that the motor with MnAl material has a wider constant power speed range and a higher rated torque than the other three IPM machines. In Fig. 19, the maximum torque attained by different magnetic materials is shown where the NdFeB obtained the highest torque value. The torque ripple, which proffers the output torque's increase along with decrease as the motor shaft rotates, is mentioned in Fig. 20. The variation in maximum and minimum torque over one complete revolution is measured in this. A medium level of torque ripple is represented by the NdFeB; similarly, a higher torque ripple was shown by the ferrite. In the motor design process, the induced EMF harmonics are mitigated to minimize the ripple torque. These harmonics are associated with the spatial distribution of the winding in conjunction with the excitation magnetic field produced by magnets.

3.5 Performance Assessment Based on Loss and Efficiency

Here, to identify the best magnetic material, the loss along with the efficacy of different magnetic materials is analogized for PMSM design. If all the output torques are well-fitted within the specified acceptable ranges, the information about the motor losses as well as operational efficacies will be the major concern in spite of the PMSM's output torque performance with varied PM materials. If all the output torques are in the acceptable range then the detailed analysis of the losses and operational efficiencies of PMSM will be a major factor.

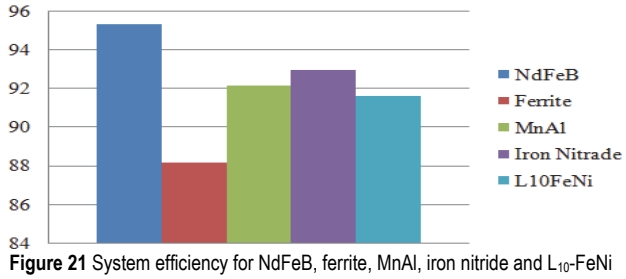

Figure 21 System efficiency for NdFeB, ferrite, MnAl, iron nitride and L_{10}-FeNi magnetic materials

As per Fig. 21, higher efficiency of 95.37% was attained by the NdFeB magnetic material in PMSM design. A lower efficiency was displayed by the ferrite magnets. When analogizing magnet loss, a lower loss of 0.3203 watts was attained by the NdFeB whereas the other materials, for instance, the ferrite attained a higher loss of 3.94. Similarly, the loss was varied for other materials also. Thus, for higher efficiency traction applications, the higher efficiency along with lower magnet loss materials will be considered. Thus, it is evident that superior performance was shown by the iron nitrade next to rare earth magnet; thus, it can be considered as a better replacement for RE metals in PMSM.

PMSMs are designed with same dimensions with different materials. Based on the market price and density of the materials, cost of the materials is compared. When contrasted with the other materials, the cost of NdFeB

material is extremely high. Conversely, a lesser cost was shown by ferrite magnets than the other materials like MnAl, Iron nitride, L_{10}FeNi magnets. The processing and making of these magnets are complicated. Thus, ferrite is established as a better material for replacing RE metals in PMSM concerning cost, loss, along with efficacy.

Table 3 Comparative analysis of different materials based on peak power, peak efficiency, active material cost, and torque density

Machine Parameters	NdFeB	Ferrite	MnAl	$Fe_{16}N_2$	L_{10}FeNi
Output Power / kW	28.4	22.8	15.04	18.67	16.54
Efficiency / %	95.33	88.13	92.16	92.99	91.59
Active material cost / $/kg	3125	1570	2987	2654	3045
Torque density / Nm/m^3	167.5	85.16	97.05	106.5	95.46

The performance of various magnetic materials utilized for the substitution of RE magnets in PMSM is evaluated in Tab. 3. The alternate best magnet is estimated regarding these metrics' efficacy along with loss comparisons. Peak power in the range of 18.67 kW and a peak efficiency of 92.99% are attained by the iron nitrade. Also, the iron nitrade's active material cost was 2654 $/kg with 106.5 Nm/m^3 torque density. Moreover, relatively higher cost along with lower power was demonstrated by the other materials. Thus, it is evident that better performance was displayed by the iron nitrade thus turning into a better material for substituting RE metals in PMSM.

4 CONCLUSION

PMSM, which is extensively utilized in automotive applications, has higher power along with torque densities. The motor is required to be operated in an extremely higher ambient temperature together with a limited space environment for automotive applications. More and more attention is gained by the PMSMs in EV applications owing to their advantages. In the field of electrical machine design, the issue of mitigating the cost as well as unstable supply of RE magnets in a PMSM is a severe complication. Consequently, to overcome these challenges, various magnetic materials like, Ferrite, Manganese Aluminide (MnAl), Iron Nitride ($Fe_{16}N_2$), Tetrataenite (L_{10}-FeNi), and Nanocomposite are utilized in this methodology as a substitute for developing Evs, thus assuring lower cost along with mass production in manufacturing. The proposed model completely examined the temperature dependent along with torque characteristics of such PM machines by utilizing PM magnets. The outcomes displayed that with elevating operational temperatures, the machine-generated torques will be down-rated; in addition, relatively best overall performance was provided by the machine with varied magnets. Moreover, when analogizing the PMSM's cost together with cogging effects for the production of EVs, it was established that the PMSM with iron nitrade PMs has 106.05 Nm/m^3 torque with a lower cost, thus providing next performance to the RE permanent magnets. Then, machine with MnAl achieves torque density of 97.05 Nm/m^3 with better efficiency that is also a good competitor to RE magnets. Although ferrite PM consumes lower cost it underperforms. In the future, by utilizing these magnetic materials with higher performance along with valuable design guidance, the proposed framework can be tested with prototype machine for operating in varied PMSM operational environments.

5 REFERENCES

[1] Wenye, W., Qingzhang, C., Xiaoyong, Z.,Qing, L., Fuzhou, Z., Jianhong, Y., & Linlin, G. (2015). Design and analysis of a new permeability modulated interior permanent magnet synchronous machine. *IEEE Transactions on Magnetics*, *57*, 1-5. https://doi.org/10.1109/TMAG.2020.3015784

[2] Yang, Y., Qiang, H., Chunyun, Fu., Shuiping, L., & Peng, T. (2020). Efficiency improvement of permanent magnet synchronous motor for electric vehicles. *Energy, 213*, 1-11. https://doi.org/10.1016/j.energy.2020.118859

[3] Xiaodong, S., Zhou, S., Gang, L., & Youguang, G. (2019). Analysis, design and optimization of a permanent magnet synchronous motor for a campus patrol electric vehicle. *IEEE Transactions on Vehicular Technology*, *68*, 10535-10544. https://doi.org/10.1109/TVT.2019.2939794

[4] Hao, C., Christopher. H., & Lee, T. (2017). Parametric sensitivity analysis and design optimization of an interior permanent magnet synchronous motor. *IEEE Access*, *7*, 159918-159929. https://doi.org/10.1109/ACCESS.2019.2950773

[5] Wenzhe, D. & Shuguang, Z. (2018). Electromagnetic vibration and noise of the permanent magnet synchronous motors for electric vehicles an overview. *IEEE Transactions on Transportation Electrification*, *5*,59-70. https://doi.org /10.1109/TTE.2018.2875481

[6] Omokhafe, J. T., Edwin, A. U., & Enesi, A. (2021). Pulse width modulation analysis of five-level inverter-fed permanent magnet synchronous motors for electric vehicle applications. *International Journal of Robotics and Control Systems*, *1*, 477-487. https://doi.org/10.31763/ijrcs.v1i4.483

[7] Zhengjie, H., Yang, Y., Yimin, G., Zhengqiang, H., Chenchen, Z., Hongda, S., & Jiannan, Z. (2021). Linear/nonlinear active disturbance rejection switching control for permanent magnet synchronous motors. *IEEE Transactions on Power Electronics*, *36*, 9334-9347. https://doi.org /10.1109/TPEL.2021.3055143

[8] Shuai, C., Jinpeng, Y., Lin, Z., & Yumei, M. (2020). Adaptive fuzzy control for permanent magnet synchronous motors considering input saturation in electric vehicle stochastic drive systems. *Journal of the Franklin Institute*, *357*, 8473-8490. https://doi.org/10.1016/j.jfranklin.2020.04.040

[9] Raihan, M., Smith, K., Almoraya, A., & Khan, F. (2017). Interior permanent magnet synchronous machine (IPMSM) design for environment friendly hybrid electric vehicle (HEV) applications. *IEEE Region 10 Humanitarian Technology Conference (R10-HTC*). https://doi.org/10.1109/R10-HTC.2017.8288978

[10] Jikai, S., Suzhen, Z., Haichao, F., Yihua, H., & Wenping, C. (2018). Analysis of temperature field for a surface-mounted and interior permanent magnet synchronous motor adopting magnetic-thermal coupling method. *CES Transactions on Electrical Machines and Systems*, *2*, 166-174. https://doi.org/10.23919/TEMS.2018.8326464

[11] Jikai, S., Suzhen, Z., Haichao, F., Ruiwu, C., & Yihua, H. (2018). Multi-objective optimization of surface-mounted and interior permanent magnet synchronous motor based on taguchi method and response surface method. *Chinese Journal of Electrical Engineering*, *4*, 67-73. https://doi.org/10.23919/CJEE.2018.8327373

[12] Tianfu, S., Jiabin, W., Chengli, J., & Lei, P. (2020). Integration of FOC With DFVC for interior permanent magnet synchronous machine drives. *IEEE Access*, *8*, 97935-97945. https://doi.org/10.1109/ACCESS.2020.2996948

[13] Md Sariful, I., Mazharul, C., Amina, S., Mohammad, I., & Iqbal, H. (2021). Multiload point optimization of interior permanent magnet synchronous machines for high-

performance variable-speed drives. *IEEE Transactions on Industry Applications*, *57*, 427-436. https://doi.org/10.1109/TIA.2020.3040141

[14] Chiranjit, S., Atanu, B., & Pabitra, K. B. (2019). Modelling and comparative dynamic analysis due to demagnetization of a torque controlled permanent magnet synchronous motor drive for energy-efficient electric vehicle. *ISA Transactions*, *97*, 1-17. https://doi.org/10.1016/j.isatra.2019.08.008

[15] Abdelli, A., Chareyron, B., & Gaussens, B. (2019). Design of a 200 kW PM synrel motor without rare-earth magnets for electric vehicle. *32nd Electric Vehicle Symposium (EVS32)*, Lyon, France. https://doi.org/10.1109/ICEM49940.2020.9270710

[16] Ping, Z., Weinan, W., Mingqiao, W., Yong, L., & Zhenxing, F. (2017). Investigation of the magnetic circuit and performance of less-rare-earth interior permanent-magnet synchronous machines used for electric vehicles. *Energies*, *10*, 1-22. https://doi.org/10.3390/en10122173

[17] Chaelim, J., Junkyu, P., & Nicola, B. (2021). Direct Drive Applications: Possible Replacement of Rare-Earth Permanent Magnet Motors. *Energies*, *14*, 1-14. https://doi.org/10.3390/en14238058

[18] Gurutz, A., Damian, C., Borja, P., Miguel, M. I., & Ibon, E. (2021). Eliminating rare earth permanent magnets on low-speed high-torque machines a performance and cost comparison of synchronous reluctance machines, ferrite permanent magnet-synchronous reluctance machines and permanent magnet synchronous machines for a direct-drive elevator system. *IET Electric Power Applications*, *15*, 1-9. https://doi.org/10.1049/elp2.12032

[19] Maria, H., Maarten, M., Omar, H., Luca, M., Oliver, W., & Joeri, V. M. (2017). Environmental impact of traction electric motors for electric vehicles applications. *The International Journal of Life Cycle Assessment*, *22*, 54-65. https://doi.org/10.1007/s11367-015-0973-9

[20] Michele, D. G., Jonathan, J., & Alessandro, Z. (2019). Designing, prototyping and testing of a ferrite permanent magnet assisted synchronous reluctance machine for hybrid and electric vehicles applications. *Sustainable Energy Technologies and Assessments*, *31*, 86-101. https://doi.org/10.1016/j.seta.2018.12.002

[21] Chae, L. J., Young, K. K., & Jin, H. (2019). Optimized design of PMSM with hybrid type permanent magnet for improving performance and reliability. *IEEE Transactions on Industry Applications*, 55, 4692-4701. https://doi.org/10.1109/TIA.2019.2924614

[22] Jong, H. W., Tae, K. B., Hoon, L., Kyong, H. K., Seung, H. S., & Jang. Y. C. (2020). Electromagnetic characteristic analysis of high-speed motors with rare-earth and ferrite permanent magnets considering current harmonics. *IEEE Transactions on Magnetics*, *57*, 1-5. https://doi.org/10.1109/TMAG.2020.3016163

[23] Xiaoyong, Z., Weiqiang, W., Quan, L., Zixuan, X., & Weiwei, G. (2018). Design and multi-objective stratified optimization of a less-rare-earth hybrid permanent magnets motor with high torque density and low cost. *IEEE Transactions on Energy Conversion*, *34*, 1178-1189. https://doi.org/10.1109/TEC.2018.2886316

[24] Wang, A., Yihua, J., & Soong, W. (2011). Comparison of Five Topologies for an Interior Permanent-Magnet Machine for a Hybrid Electric Vehicle. *IEEE Transactions on Magnetics*, *47*, 3606-3609. https://doi.org/10.1109/TMAG.2011.2157097

[25] Zefan, S. & Shenqiang, R. (2020). Rare-earth-free magnetically hard ferrous materials. *Nanoscale Adv*, *2*, 4341-4349. https://doi.org/10.1039/D0NA00519C

[26] Yawei, W., Nicola, B., & Ronghai, Q. (2022). Comparative Study of Non-Rare-Earth and Rare-Earth PM Motors for EV Applications. *Energies*, *15*, 711. https://doi.org/10.3390/en15082711

[27] Hamed, T., Mehdi, A., & Jawad, F. (2020). Ferrite Permanent Magnets in electrical Machines: Opportunities and Challenges of a Non-Rare-Earth Alternative. *IEEE Transactions on Magnetics*, *56*, 1-20. https://doi.org/10.1109/TMAG.2019.2957468

[28] Hailiang, F., Sofia, K., Jonas, A., Johan, C., Peter, S., Klas, G., & Martin, S. (2016). Directly obtained τ-phase MnAl, a high performance magnetic material for permanent magnets. *Journal of Solid State Chemistry*, *237*,300-306. https://doi.org/10.1016/j.jssc.2016.02.031

[29] Tuvshin, D., Ochirkhuyag, T., Hong, S., & Odkhuu, D., (2021). First-principles prediction of rare-earth free permanent magnet: FeNi with enhanced magnetic anisotropy and stability through interstitial boron. *AIP Advances*, 11, 015138. https://doi.org/10.1063/9.0000127

[30] Kurichenko, V. L., Karpenkov, D. Y., Karpenkov, A. Y., Lyakhova, M. B., & Khovaylo, V. (2019). Synthesis of FeNi tetrataenite phase by means of chemical precipitation. *Journal of Magnetism and Magnetic Materials*, *470*, 33-37. https://doi.org/10.1016/j.jmmm.2017.11.040

[31] Lama, R., Farah, F., Khulud, H., Nader, Y., & Ramadan, A. (2021). Exchange spring behaviour in $BaFe_{12}O_{19}/CoFe_2O_4$ magnetic nanocomposites. *Journal of Alloys and Compounds*, *868*, 159072. https://doi.org/10.1016/j.jallcom.2021.159072

Contact information:

Sundaramahalingam SUBRAMANIAM, Assistant Professor (Sr.Grade)
(Corresponding author)
Mepco Schlenk Engineering College,
Tamilnadu, India, 626005
E-mail: sundar.eee@mepcoeng.ac.in

Manikandan Bairavan VEERAYAN, Senior Professor
Mepco Schlenk Engineering College,
Tamilnadu, India, 626005
E-mail: bvmani@mepcoeng.ac.in